Cancer Cell International

RESEARCH Open Access

TNS4 promotes lymph node metastasis of gastric cancer by interacting with integrin B1 and inducing the activation of fibroblastic reticular cell

Xiang Zhang[1†], Guang-Hong Su[1†], Tian-Shang Bao[2†], Wei-Pai He[2†], Yang-Yang Wang[2†], Yao-Qi Zhou[1†], Jia-Xuan Xie[1], Fei Wang[2], Rui Lu[1], Shan Zhang[1], Shuang-Qin Yi[3], Qing Li[1], Shu-Heng Jiang[1], Hui Li[1*], Li-Peng P. Hu[1*], Jun Li[1*] and Jia Xu[2*]

Abstract

Lymph node (LN) metastasis of gastric cancer (GC) is one of the important pathways of GC metastasis, indicating the clinical staging and prognosis of patients. To investigate the underlying mechanism during the process of GC-induced LN metastasis, 7 pairs of GC tissues, paracancerous (PC) tissues, GC-positive LN (LN.P) and GC-negative LN (LN.N) tissues from GC patients with homogeneity were selected for RNA sequencing (RNA-seq) analysis. Tensin 4 (TNS4) was screened out and found to be significantly upregulated in LN.P tissues and closely related with the characteristics of GC. In vitro and in vivo experiments demonstrated that knockdown of TNS4 could significantly inhibit LN metastasis of GC cells and activation of fibroblastic reticular cells (FRCs) in LNs, thus inhibiting LN expansion induced by tumor cell invasion. Moreover, TNS4 was found to be interacted with integrin beta 1 (ITGB1) on FRCs, thereby affecting the binding of transforming growth factor β1 (TGF-β1) to ITGB1 and subsequently regulating downstream signaling molecules, and supporting the GC cell-induced LN metastasis.

Keywords Gastric cancer, Lymph node metastasis, Fibroblastic reticular cells, Tensin 4, Integrin beta 1

†Xiang Zhang, Guang-Hong Su, Tian-Shang Bao, Wei-Pai He, Yang-Yang Wang and Yao-Qi Zhou contributed equally to this work.

*Correspondence:
Hui Li
huili@shsci.org
Li-Peng P. Hu
lphu@shsci.org
Jun Li
junli@shsci.org
Jia Xu
xujia201800@126.com
[1]State Key Laboratory of Systems Medicine for Cancer, Ren Ji Hospital, School of Medicine, Shanghai Cancer Institute, Shanghai Jiao Tong University, Shanghai, China
[2]Department of Gastrointestinal Surgery, Renji Hospital, School of Medicine, Shanghai Jiao Tong University, Shanghai, China
[3]Department of Frontier Health Sciences, Graduate School of Human Health Sciences, Tokyo Metropolitan University, Hachioji, Japan

Introduction

According to Cancer Statistics in 2020, gastric cancer (GC) is one of the most common malignant digestive system tumors, ranking sixth in the global incidence rate and third in mortality respectively [1]. The disease is prevalent in East Asian countries such as China, Japan, and South Korea [2]. The pathogenesis of GC is relatively insidious and invasive, leading to a diagnosis at advanced stages, often accompanied by distant organ metastases such as the liver [3–6]. Lymph node (LN) metastasis of GC is one of the important pathways of metastasis, usually occurring in a proximal to distal or skip manner [7–10]. The LN metastasis status of GC indicates the clinical staging and prognosis of patients and has important guiding significance for corresponding treatment in clinical practice [11, 12]. Therefore, clarifying the molecular mechanisms related to LN metastasis in GC and exploring effective diagnostic and treatment methods are essential for improving the prognosis of GC.

Tensin was identified as a protein that maintains the tension of actin filaments [13]. Until now, four members of the tensin family have been found in mammals, namely the earliest discovered tensin 1 (TNS1), as well as three other tensin 2 (TNS2), tensin 3 (TNS3), and tensin 4 (TNS4) discovered for new tensin family members with broad sequence homology to TNS1 [14–17]. These four members of the tensin family all contain the SH2 functional domain and phosphotyrosine binding domain at the C-terminus, which enables tensin to interact with key molecules on multiple signaling pathways. The TNS family proteins also play crucial roles in the occurrence and development of tumors. While evidence suggests that TNS2 has an inhibitory effect on tumors, the correlation between TNS1-3 expression and carcinogenic effects, especially in colorectal cancer (CRC) and pancreatic ductal adenocarcinoma (PDAC), has potential clinical significance [18, 19]. Recent reports have demonstrated that TNS4 expression in esophageal squamous cell carcinoma (ESCC) is regulated by the transcription of Epidermal Growth Factor receptor (EGFR) and mitogen-activated protein kinase (MAPK) pathways [20]. In addition, studies have shown that TNS4 is stimulated by KRASG12D and SRY-related HMG box transcription factor 17 (SOX17) in intrahepatic cholangiocarcinoma (ICC), thereby exerting its role in promoting tumor occurrence and development [21]. However, there have been few reports on the function and role of TNS4 in LN metastasis of GC until now. The underlying molecular mechanism is still unclear.

In this study, we performed quantitative real-time quantitative PCR (qPCR) and Western Blotting on human patient tissues, founding that TNS4 gene is significantly upregulated in GC-positive LN (LN.P) tissues compared to GC-negative LN (LN.N) tissues, and investigated the biological functions of TNS4 in LN metastasis of GC. Then, in vitro experiments using mouse cell lines and in vivo experiments using mouse models demonstrated the promotive effects of TNS4 on the process of LN metastasis in GC. We used foot pad-tumor induced LN metastasis model for in vivo experiments, a commonly used LN metastasis model [22]. By injecting tumor cells into the mouse foot pad and collecting draining lymph nodes (DLNs), tumor inducedLN metastasis can be evaluated by comparing the size of LNs. Moreover, TNS4 was found to play an important role in regulating the TGF-β1 related signaling pathway by interacting with ITGB1, thus promoting LN metastasis in GC.

Methods

Regents

The primary antibodies used in the experiment include TNS4 (11580-1-AP, Proteintech, China), ITGB1(12594-1-AP, Proteintech, China), SMAD2(200790, ZEN-BIOSCIENCE, China), SMAD3(R22774, ZEN-BIOSCIENCE, China), p-SMAD2(R22952, ZEN-BIOSCIENCE, China), p-SMAD3(380775, ZEN-BIOSCIENCE, China), AKT(R23411, ZEN-BIOSCIENCE, China), p-AKT(R22961, ZEN-BIOSCIENCE, China), TGF-β1(R22797, ZEN-BIOSCIENCE, China).

Patients' enrollments and samples

To enroll patients, strict inclusion and exclusion criterias were carried out. Inclusion criteria: (1) Pathological diagnosis: GC patients were diagnosed preoperative histopathologically or cytologically; (2) Treatment status: The patients did not receive any preoperative radiotherapy or chemotherapy treatment; (3) Informed consent: The patients voluntarily participated and signed an informed consent form; (4) Clinical data: There were relatively complete clinical data and information on diagnosis and treatment. Exclusion criteria: (1) There was no clear pathological result to prove GC, and pathology cannot distinguish it clearly; (2) There were no detailed imaging evaluation results and treatment status; (3) The patients were in poor physical condition, or unable to tolerate relevant examinations or surgeries, or in poor basic physical conditions affecting prognosis, or having serious postoperative complications. Based on the above inclusion and exclusion criteria, the clinical pathological data and prognosis information of patients were statistically analyzed.

7 pairs of fresh human GC tissues, paracancerous (PC) tissues, LN.P and LN.N tissues from GC patients, were collected from the Department of Gastrointestinal Surgery, Renji Hospital, School of Medicine, Shanghai Jiao Tong University. All patients had not received radiotherapy, chemotherapy or other related anti-tumor therapies before surgery. These 7 pairs of samples were used for RNA sequencing (RNA-seq). Besides, there are other 2

unpaired fresh GC tissues and metastatic LN tissues collected from Renji hospital, together with 7 pairs of tissues mentioned before, constituting 9 cases used to perform qPCR. In addition, GC-induced LN metastatic tissue microarrays, used to perform Immunohistochemistry (IHC), containing 200 cases of formalin- preserved GC - PC - metastatic/non-metastatic LN tissues collected from Renji hospital.

The study was approved by the Research Ethics Committee of Renji Hospital, School of Medicine, Shanghai Jiao Tong University. Written informed consent was provided before enrollment. Approval letter of Shanghai Jiaotong University School of Medicine, Renji Hospital Ethics Committee is KY2024-046-C.

RNA-seq

RNA-seq was performed to detect these 7 pairs of clinicopathological samples and analyze genes differentially expressed during the process of GC-induced LN metastasis. Total RNA of samples was isolated using TRIzol reagent for RNA sequencing according to the manufacturer's instructions. All samples were sent to Tiangen Biotech Co., Ltd. (Beijing, China) and the standard RNA-seq process was carried out.

The RNA-seq data from this study have been deposited on the NCBI (http://www.ncbi.nlm.nih.gov/) database under the umbrella BioProject PRJNA1160027.

Cell culture

The mouse GC cell line mouse forestomach carcinoma (MFC) cells were cultured in RPMI 1640 (L210KJ, Basal Media, China). The cell culture system was supplemented with 10% FBS (DCF-201-0500, Dcell, China) and 1% penicillin/streptomycin (S110JV, Basal Media, China). Cells were cultured at 37 °C in a humidified chamber with 5% CO2.

Cell co-culture

Transfect sh-TNS4 plasmid into MFC cells. After 48 h of transfection, lay a 24-well plate. Set groups as vehicle group, FRCs + sh-NC MFC, FRCs + sh-TNS4 MFC. The cell density in each well is 2000 cells per well. After 48 h of co-cultivation, tale visible light and then perform immunofluorescence staining.

Transfect si-ITGB1 into FRC cells and si-TNS4 into MFC cells. After 48 h of transfection, lay in a 6-well plate. 48 h later, partial digestion was performed using 0.05% trypsin to digest FRCs and then extract protein. The experimental groups were set as FRCs + MFC, si-NC FRCs + si-NC MFC, si-NC FRCs + si-TNS4 MFC, si-ITGB1 FRCs + si-NC MFC, si-ITGB1 FRCs + si-TNS4 MFC.

Cell transfection

Before transfection begins, the culture medium of each well was replaced with a fresh serum-free culture medium. Taking the transfection of a single well as an example, prepare a 1.5 ml sterile centrifuge tube. Then, 2 μg of the shRNA was diluted with 200 μl of jetPRIME ® Buffer (101000046, Polyplus transfer, France). Then 5 μl of reagent was added into the buffer. Vortex again for 10 s, invert and mix well. 200 μl transfection mixed solution was added to each transfection well. After 4–6 h, the culture medium of each well was replaced with a fresh culture medium containing 10% FBS (DCF-201-0500, Dcell, China). Perform functional experiments 48 h after transfection.

Western blotting

RIPA lysate (YSD0100, Yoche, China) *were used* to extract protein. Add 5 × loading buffer (WB2001, NCM, China) to each centrifuge tube and soak in a water bath at 100 ℃ for 10 min. Electrophoresis at 80 V for 30 min and at 120 V for 60 min, followed by SDS-PAGE electrophoresis to separate protein extracts. The membranes were sealed with 5% skim milk powder (232100, BD, USA) at room temperature for 1 h. Incubate primary antibody overnight at 4℃. Incubate secondary antibody at room temperature for 1 h. Bands were developed using luminescent liquid (P10300, NCM, China).

In this study, TNS4 expression level was evaluated in fresh human GC tissues by western blotting. And then, TNS4 knockdown efficiency was evaluated in mouse GC cell lines (MFC) by western blotting. Besides, the expression level of p-SMAD2, SMAD2, p-SMAD3, SMAD3, TGF - β 1, p-AKT and AKT in mouse FRCs were assessed by western blotting.

qPCR

RNA was extracted using trizol (9109, Takara, Japan) and stored at -80℃. Use the 2 Step Real-time RT-PCR kit (RR036A, Takara, Japan) for reverse transcription of RNA. Configure the 10 μl reverse transcription system according to the instructions and perform the reverse transcription reaction at 37 °C for 15 min and 85 °C for 5 s. The DNA was stored at -20℃. Perform qPCR reaction using the 2X Universal Blue SYBR Green qPCR Master Mix Kit (G3326, servicebio, China). qPCR reaction was conducted in ViiA ™ 7 (Applied Biosystems ™, USA). The cyclic parameters consisted of an initial hotstart step at 95 °C for 30 s, followed by 40 repetitions of 95 °C for 15 s and 60 °C for 30 s. The melting curve was set according to the instrument's default settings. The primers used in the experiment are shown in the table below. The data is calculated using the following formula: (1) ΔCq = Cq (sample) - Cq (reference) (2) ΔΔCq = Δ Cq (sample) - Δ Cq (calibrator) (3) Fold change = 2^(-ΔΔCq).

In this study, the expression level of TNS4 was assessed in fresh human GC tissues using qPCR. Subsequently, the knockdown efficiency of TNS4 was evaluated in the mouse GC cell line (MFC) via qPCR.

TNS4-F(human)	AGCCAGGGGCTTTTGTCATAA
TNS4-R(human)	AGACGACTCGATGAGGAAGTG
TNS4-F(mouse)	TGTCCTTACTACACCACAGAGAG
TNS4-R(mouse)	CCAGGGAGAAGTCAATGCAAG
α-SMA-F(mouse)	GTCCCAGACATCAGGGAGTAA
α-SMA-R(mouse)	TCGGATACTTCAGCGTCAGGA
Col1a1-F(mouse)	TTCTCCTGGCAAAGACGGAC
Col1a1-R(mouse)	CTCAAGGTCACGGTCACGAA

Immunohistochemistry staining

The samples were placed on a 60℃ baking machine for 1 h of dewaxing. The samples were hydrated according to the steps. The slides were put into a sodium citrate solution, boiling for 10 min. The samples were treated with 3% H_2O_2 for 30 min. The samples were sealed at room temperature with 10% BSA for 1 h. Drop 100 μl of primary antibody onto each sample in a wet box and incubate overnight at 4 ℃. Drop 200 μl of secondary antibody onto the samples in a wet box and incubate at room temperature for 1 h. Prepare DAB solution (SB-D6077, Share-Bio, China) according to the instructions. 100 μl of DAB was added to each slide, and react for 10 s. Dehydrate the samples according to the steps. Seal with neutral resin [4, 23, 24].

For IHC experiment, negative control and positive control were set in advance. Primary antibodies were replaced with PBS as negative controls. Positive expression samples were used as positive controls.

Each sample was evaluated by this rule: according to the proportion of positive areas, it is divided into 0–3 points, 0–5% for 0 points, 5–30% for 1 point, 30–60% for 2 points, and 60–100% for 3 points, 0 and 1 were considered as low expression level, 2 and 3 were considered as high expression level.

In this study, TNS4 expression was first evaluated in human GC microarrays using IHC and subsequently assessed in mouse lymph node (LN) tissues by IHC. Additionally, the expression levels of α-SMA, Sirius Red, and ITGB1 in mouse LN tissues were also evaluated using IHC.

Immunofluorescence (IF)

Discard the culture medium from the 24-well plate and wash with PBS three times for 5 min each time. Fix at room temperature with 4% paraformaldehyde (P1110, Solarbio, China) for 30 min. The wells were perforated with PBS containing 0.1% triton X-100 (T8200, Solarbio, China) for 10 min. The wells were then sealed at room temperature with 5% BSA (4240GR005, biofroxx, Germany) for 1 h. The wells were incubated with primary antibody overnight at 4 °C, and then incubated with secondary antibody at room temperature for 1 h. Finally, 200 μl 10 μg/μl DAPI solution were added to each well, incubating at room temperature for 10 min. Extract the cell slides and seal them with an anti-fluorescence quenching agent (S2100, Solarbio, China). The immunofluorescence slides were temporarily stored at 4℃ and captured using a confocal microscope within a week.

Co-immunoprecipitation (Co-ip)

For HA-based immunoprecipitation, cell lysates of mice fibroblasts transfected with HA-tagged TNS4 or control were subjected to immunoprecipitation with anti-HA monoclonal antibody (05-904, Millipore, USA) or control IgG overnight and then incubated with protein A/G magnetic beads (Invitrogen, 10003D, USA) over night at 4 °C. The beads were washed three times in lysis buffer, after which the immunoprecipitated protein complexes were resuspended in 2 × loading buffer followed by western blot analysis.

TGF-β1 neutralization

TGF-β1 neutralizing antibody (Monoclonal Antibody 2E6, Invitrogen, USA) was used to treat FRCs which were co-cultured with MFC cells at a concentration of 10 μg/ml (1:100).

Mouse model

Mouse model was used to explore the function of TNS4 in shorter time rather than using human model. 6–8 weeks of C57BL6/J male mice were purchased from Shanghai Jiesijie Experimental Animal Co., Ltd, and randomly grouped. We made sure that the weight and physiological condition of mice in each group were the same. The animal experiments were approved by the Renji Hospital Animal Ethics Committee (ID: 2024-066).

To investigate the role of TNS4 during the process of GC-induced LN metastasis, MFC cells were selected, a mouse-derived GC cell line with high expression level of the TNS4 gene for the experiment. Before injection, TNS4 gene was knocked down using shRNA in MFC cells, and the interference efficiency of TNS4 was detected by western blotting or real-time PCR. By injecting 25 μl MFC cells into mouse footpads, a LN metastasis model in C57BL6/J mice was created. The control group was injected with MFCs-NC cells, while the experimental group was injected with MFCs-sh-TNS4 cells. All mice were euthanized by spinal dislocation after carbon dioxide anesthesia. The distal DLNs, located at the inguinal region of mice, were collected for observation at 7 day and 15 day after inoculating the tumor cells. Sample size calculation followed this rule: Volume = length * width^2 /2.

To investigate the function of ITGB1 on TNS4, ITGB1 inhibitors were injected into mouse fat pads on day 0, day 5, and day 10, respectively. The groups were set as: MFC-vehicle group, MFC-sh-TNS4 group, inhibitor group and MFC-shTNS4 + inhibitor group. MFC-vehicle group was set as the control group. Mouse DLNs were collected on day 7 and day 15. Photos were taken and the size of each lymph node were measured.

Statistical analysis

If there are no special instructions, data were presented as the means ± standard errors of the mean (SEMs). The statistical analyses of the characteristics of GC were done using SPSS 16.0 for Windows (IBM). Other statistical analyses were performed using GraphPad Prism 5 for Windows. One-way ANOVA or two-tailed Student's t test was used for comparisons between groups. Values of $P < 0.05$ were considered statistically significant.

Results

TNS4 was up-regulated in GC metastatic LN tissues and closely related with the characteristics of GC

In this research, we selected 7 pairs of tissue samples from GC patients with homogeneity (similar pathological features such as primary lesion infiltration, LN metastasis, WHO pathological classification, etc.) for RNA-seq analysis. Each pair of tissue samples included GC tissues, PC tissues, LN.P and LN.N tissues.

To identify the key molecule driving LN metastasis of GC, RNA sequencing was performed to detect these 7 pairs of clinicopathological human patient samples and analyze genes differentially expressed during the process of GC-induced LN metastasis (BioProject: PRJNA1160027) (**Supplemetary** Table 1). We found that the expression of the TNS4 gene was significantly up-regulated in human GC and GC metastatic LNs, compared to PC and GC non-metastatic LN tissues (Fig. 1A). To validate these findings, we performed qPCR on human GC - PC- metastatic/non-metastatic LN tissues. It was found that TNS4 was significantly up-regulated in GC metastatic LN tissues (Fig. 1B **and C**). To further investigate the expression level of TNS4 in tissues, we used western blotting to detect the expression of TNS4 protein in 3 pairs of human GC - PC - metastatic/non-metastatic LN tissues. We found that TNS4 was upregulated in GC and metastatic LN tissues, especially in metastatic LN tissues (Fig. 1D **and E**). These results demonstrated that TNS4 is significantly up-regulated during the process of LN metastasis in GC.

To further investigate TNS4 expression, we performed IHC staining on human patient GC-induced LN metastatic tissue microarrays (containing 200 cases of GC - PC - metastatic/non-metastatic LN tissues). It was revealed that TNS4 showed high expression in both GC and metastatic LN tissues compared to PC tissues and LN. N tissues (Fig. 1F). The high expression was especially obvious in LN.P tissues that underwent invasive metastasis of GC. Meanwhile, a comparison between TNS4 in metastatic LN and non-metastatic LN tissues of GC showed that TNS4 was significantly up-regulated in 71.15% of all metastatic LN tissues (Fig. 1G). Human patient LN tissues' pathological characterization revealed that the expression of TNS4 was closely associated with LN metastasis as well as TNM staging in GC patients, suggesting that TNS4 might play an important regulatory role in the process of LN metastasis in GC (Table 1). Meanwhile, the Multivariable risk factor analysis also indicated that TNS4 was closely correlated with T factor of TNM staging in GC patients (Table 2).

Knockdown of TNS4 inhibits GC cell-induced LN metastasis and FRC activation in vivo

By injecting MFC cells into mouse footpads, we constructed a LN metastasis model in C57BL6/J mice. We collected the distal DLNs for observation at 7 day and 15 day after inoculating the tumor cells (Fig. 2A). Before injection, we knocked down TNS4 using shRNA in MFC cells, and the interference efficiency of TNS4 was detected by western blotting or real-time PCR (Fig. 2B). Then TNS4 silenced and control MFC cells were inoculated into the footpad of 5–6 weeks old C57BL6/J mice respectively, and the DLNs were collected at day 7 and day 15. It was found that the knockdown of TNS4 significantly suppressed the expansion of DLNs induced by the MFC cells (Fig. 2C). Statistical analyses also indicated that the knockdown of TNS4 could inhibit the increase of LN volume and weight (Fig. 2D **and E**). To clarify the localization of TNS4 in LNs, we performed immunofluorescence (IF) staining of metastatic LN tissues at 15 day. The results revealed co-localization of TNS4 and pan-cytokeratin (pan-CK), indicating that TNS4 expression was mainly localized on tumor cells invading and metastasizing into LNs (Fig. 2F).

Moreover, by performing IHC staining and Sirius red staining of *those mouse* LN tissues at 15 day, we found that the expression of pan-CK, the marker indicating the status of metastatic GC cells, was significantly decreased in the LN tissues of the TNS4-silenced group compared with that in the control group. A reduction in TNS4 expression was also observed (Fig. 2G **and H**). In addition, the expression of a-SMA and extracellular collagen deposition were found to be decreased, indicating that the activation status of fibroblastic reticular cells (FRCs), which determines the degree of LN swelling, was significantly reduced (Fig. 2I **and J**). These results suggested that knockdown of TNS4 could significantly inhibit LN metastasis of GC cells and activation of FRCs in LNs,

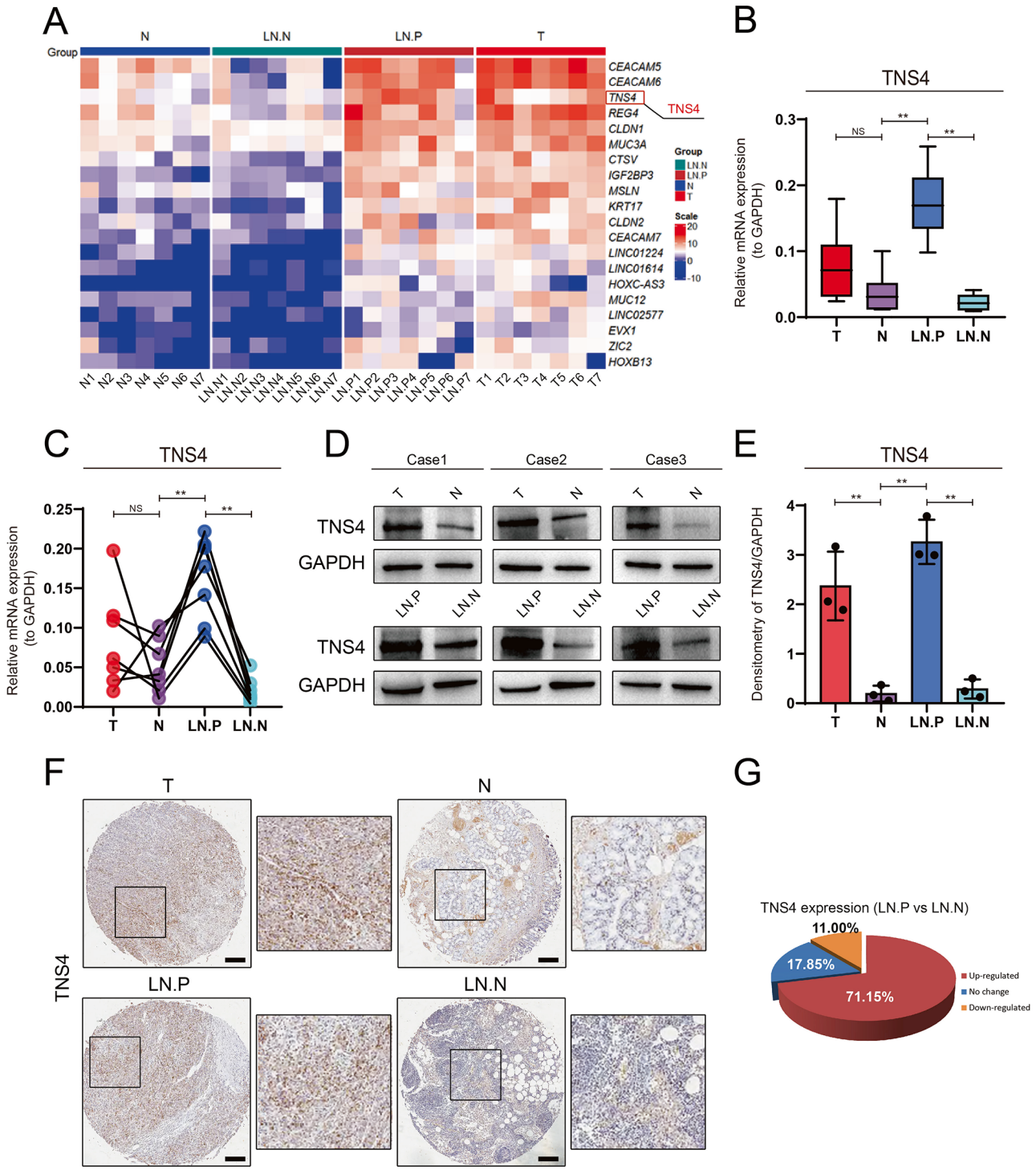

Fig. 1 TNS4 was up-regulated in GC tissues and especially had a high expression in tumor cells invaded LNs. (**A**). RNA-seq analysis of 7 pairs of clinical samples of GC, PC, LN.P and LN.N tissues; (**B**). The mRNA expression of TNS4 in GC, PC, LN.P and LN.N tissues; (**C**). The mRNA expression of TNS4 in 7 paired GC, PC, LN.P and LN.N tissues; (**D** and **E**). The protein expression of TNS4 in 3 paired GC, PC, LN.P and LN.N tissues (**D**). The statistical result of TNS4 expression in the 3 pairs of tissues is shown on the right (**E**); (**F**). IHC staining of TNS4 in GC-induced LN metastatic tissue microarray (containing 200 cases of GC - PC - metastatic/non-metastatic LN tissues). Scale Bar: 200 μm; (**G**). The expression changes of TNS4 in GC-induced metastatic/non-metastatic LN tissues. *$P < 0.05$;** $P < 0.01$;NS: no significance

Table 1 Analysis of TNS4 expression and pathological characteristics of clinical GC and LN metastasis tissues (Pearson's X2 test was used)

Clinicopathological Features		Total	TNS4 expression		P-value (Chi-square)
			Low	High	
		179	60	119	
Gender	Male	119	39	80	0.7658
	Female	60	21	39	
Age	≤60	74	25	49	0.9499
	>60	105	35	70	
Tumor Location	antrum/pylorus	59	17	42	0.1185
	cardia/fundus	10	2	8	
	body	26	10	16	
	lesser curvature	22	12	10	
	greater curvature	7	4	3	
	others	55	15	40	
Lymph-node invasion	N1	57	11	46	**0.0181***
	N2	73	31	42	
	N3	49	18	31	
T Factor	T1/T2	46	26	68	0.0807
	T3/T4	85	34	51	
pTNM	I	31	4	27	**0.0227***
	II	63	22	41	
	III	85	34	51	

TNM: tumor / regional lymph node / metastasis defined by American Joint Committee on Cancer (AJCC);

T: Tumor, represents the condition of the primary tumor;

N: Lymph node, represents the involvement of regional lymph nodes;

M: Metastasis, represents the situation of distant metastasis

Table 2 Multivariable risk factor analysis of TNS4 expression and pathological characteristics of clinical GC and LN metastasis tissues (Pearson's X2 test was used)

Multivariable risk factor	Hazard ratios	95% CI	*P* value
TNS4 expression in LN (high vs. low)	0.7292	0.4257 to 1.264	0.2527
Gender(male vs. female)	1.649	0.8532 to 3.465	0.1581
Age (>60 vs. <=60)	2.236	1.206 to 4.413	**0.0144***
T Factor (T3/T4 vs. T1/T2)	5.277	2.129 to 17.59	**0.0015***
LN (N2/3 vs. N1)	2.449	0.5353 to 12.53	0.2437
Location (antrum/pylorus vs. other place)	0.7163	0.3843 to 1.275	0.2721

thus inhibiting LN expansion induced by tumor cell invasion.

Silencing of TNS4 inhibits GC cell-induced FRC activation in vitro

During the process of GC cell-induced LN metastasis, FRCs are activated, leading to alterations in the internal microenvironment and consequent LN expansion. To investigate the functional role of TNS4 in the interaction between GC cells and FRCs, we isolated primary FRCs from mouse LNs and co-cultured with MFC cells (the TNS4-silenced group and the control group) (Fig. 3A). The results of visible light and a-SMA staining showed that co-culture of MFC cells with FRCs significantly led to the activation of FRCs, while knockdown of TNS4 in MFC cells significantly inhibited the activation of FRCs (Fig. 3B **and C**). After observing the fully activated and partially activated FRCs in visible light images, it was also found that the knockdown of TNS4 in MFC could inhibit the activation of FRCs (Fig. 3D). Furthermore, real-time PCR was used to detect the FRC activation-related characteristic genes such as a-SMA and Col1a1 after obtaining the FRCs of each group through stepwise digestion. It was found that co-culture of MFC cells with FRCs resulted in a significant upregulation of a-SMA and Col1a1, which could be attenuated by knockdown of TNS4 (Fig. 3E **and F**). All these data indicated that TNS4 is involved in the interaction between GC cells and FRCs.

TNS4 directly interacts with ITGB1

To explore the underlying mechanism by which TNS4 contributes to GC cell-induced LN metastasis, we first predicted and screened on the protein interaction website (STRING: functional protein association networks (string-db. org)) and found that there is an interaction between TNS4 and integrin beta1 (ITGB1) (Fig. 4A), which was then validated through Co-IP experiments in mouse fibroblasts (Fig. 4C). Meanwhile, the direct interaction between TNS4 and ITGB1 was analyzed by HDOCK (http://hdock.phys.hust.edu.cn/). The interac tion between TNS4 and ITGB1 occurs in three regions. Through residue analysis of the docking interface, we have identified the contacts between multiple key amino acid residues. The key residues of TNS4 include MET 715, PRO 656, and HIS 583, which form strong interactions with specific amino acid residues of ITGB1 (such as ASN 411, GLN 4, ILE 740) (Fig. 4B). In addition, IF staining was performed in the LN tissues of MFC cells inoculated control group mice. It was found that TNS4 and ITGB1 had an obvious co-localization at the border where tumor cells and FRCs contacted with each other (Fig. 4D). Moreover, we observed that TNS4 was predominantly concentrated on tumor cells invading LNs, while ITGB1 was mostly localized in regions dominated by FRCs and with less aggregation of immune cells. At the forefront of tumor cell invasion, some tumor cells came into contact with FRCs, accompanied by the interaction between TNS4 and ITGB1, thus resulting in the following effects (Fig. 4E).

We further performed IHC staining of ITGB1 in the human GC-induced LN metastatic tissue microarrays and combined it with the previous results of TNS4

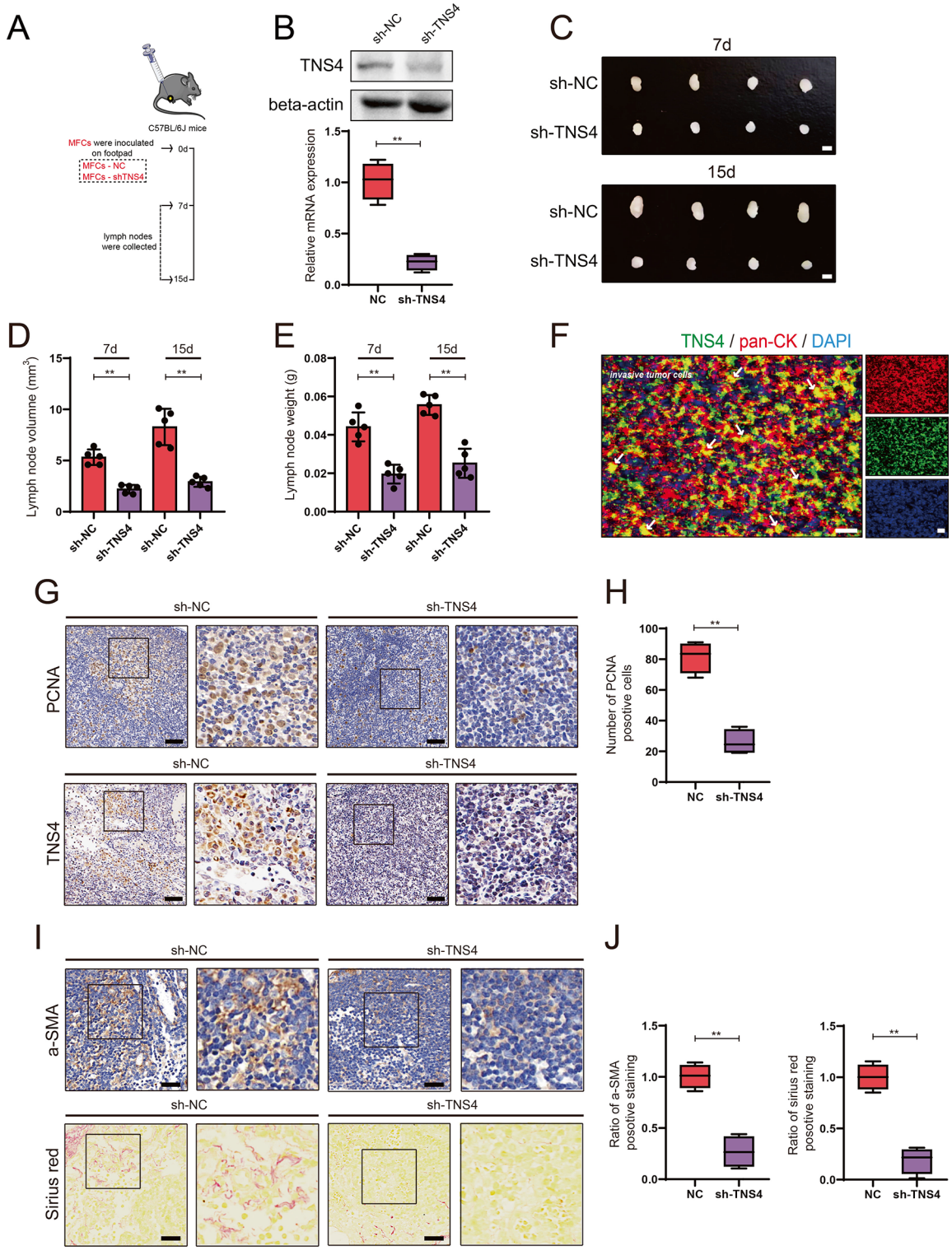

Fig. 2 Knockdown of TNS4 suppressed the LN metastasis of GC and decelerated the activation of FRCs and expansion of LNs. (**A**). Construction of a mouse foot pad LN metastasis model; (**B**). Validation of the interference efficiency of TNS4 in MFC cells; (**C**). The morphology of LN tissues from mice injected with TNS4 silenced and control MFC cells at 7 and 15 days respectively. Scale Bar: 1 mm; (**D** and **E**). Changes of LN tissue volume (**D**) and weight (**E**) between TNS4 silenced and control group at 7 and 15 days; (**F**). IF staining of TNS4 and pan-CK in LN tissues from mice of control group; (**G** and **H**). IHC staining of PCNA and TNS4 in LN tissues of TNS4 silenced and control group at 15 days (**G**). The statistical result of the number of PCNA-positive cells is shown on the right (**H**). Scale Bar: 200 μm; (**I** and **J**). IHC staining of a-SMA and Sirius Red staining in LN tissues of TNS4 silenced and control group at 15 days (**I**). The statistical results of the ratio of a-SMA and Sirius Red positive staining are shown on the right (**J**). Scale Bar: 200 μm; $^{**}P < 0.01$

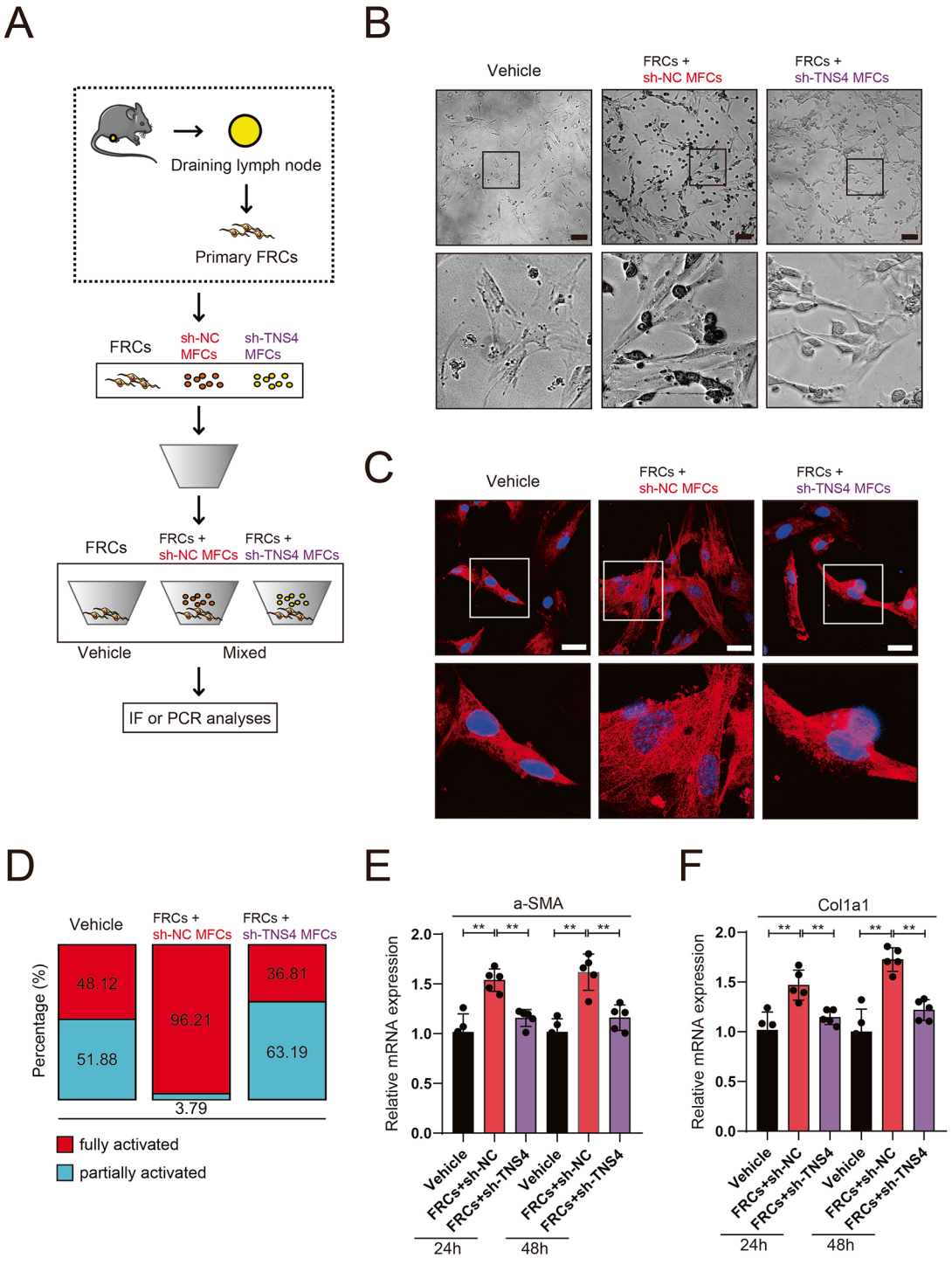

Fig. 3 GC cells derived TNS4 promoted the activation of FRCs and invasion of tumor cells. (**A**). Experimental procedure for co-culturing mouse primary FRCs with TNS4 silenced and control MFC cells; (**B**). The activation status of FRCs under the conditions of FRCs alone, FRCs co-cultured with TNS4 silenced and control MFC cells (visible light). Scale Bar: 50 μm; (**C**). IF staining of a-SMA in FRCs alone, RCs co-cultured with TNS4 silenced and control MFC cells. Scale Bar: 25 μm; (**D**). The ratio of fully activated and partially activated FRCs under the conditions of FRCs alone, FRCs co-cultured with TNS4 silenced and control MFC cells (FRCs with an overall extension length > 50 μm are considered fully activated, and FRCs with an overall extension length < 50 μm are considered partially activated); (**E** and **F**). The changes of a-SMA (**E**) and Col1a1 (**F**) mRNA expression in FRCs alone, FRCs co-cultured with TNS4 silenced and control MFC cells respectively $^{**}P < 0.01$

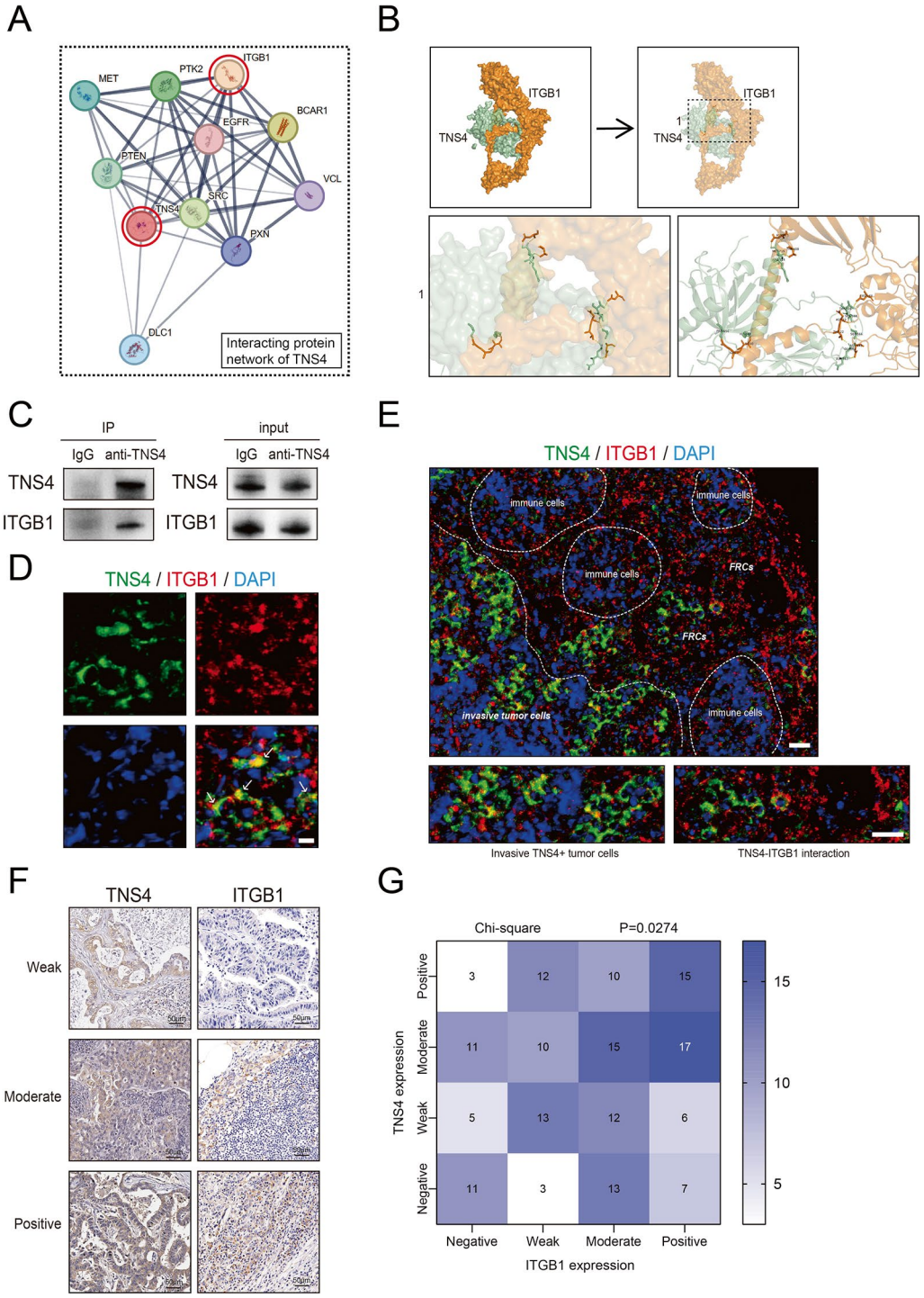

Fig. 4 TNS4 directly interacted with ITGB1. (**A**). Prediction of TNS4 interacting proteins, including ITGB1; (**B**). The direct interaction between TNS4 and ITGB1 was analyzed by HDOCK; (**C**). Co-IP verification of the interaction between TNS4 and ITGB1; (**D**). IF staining of the co-localization of TNS4 and ITGB1 in mouse LN tissue (control group). Scale Bar: 50 μm; (**E**). IF staining of the co-localization of TNS4 in tumor cells and ITGB1 in FRCs (control group). Scale Bar: 100 μm; (**F**). IHC staining analysis of the correlation between TNS4 and ITGB1 in GC-induced LN metastatic tissue microarray. Scale Bar: 50 μm; (**G**). Heatmap of the correlation analysis of the staining intensity of TNS4 and ITGB1 on a GC-induced LN metastatic tissue microarray. Data were analysed by the chi-square test. ($n = 163$, $P = 0.0274$)

staining. The analysis revealed a high correlation between the expression levels of TNS4 and ITGB1 in LN metastatic tissues (Fig. 4F). Based on the GC-induced LN metastatic tissue microarray analysis, the heatmap of the correlation analysis of the TNS4 and ITGB1 staining intensity confirmed that TNS4 was closely correlated with ITGB1 (Fig. 4G). Moreover, the Multivariable risk factor analysis indicated that ITGB1 was closely correlated with T factor of TNM staging in GC patients (**Supplemetary** Table 2).

TNS4 - ITGB1 axis regulates TGF-β1 related signaling pathways

To uncover the underlying molecular mechanisms, we conducted RNA-seq analysis on the TNS4 silenced and control *human* GC cells and found that the changes of TNS4 expression may be correlated with the integrin binding and TGF-β signaling pathway (BioProject: PRJNA1160027). We concluded that TNS4 may have a pivotal regulatory effect on these pathways in the microenvironment of GC and GC-induced LN metastasis (Supplementary Fig. 1A and B).

Through western blotting detection of FRCs under the conditions of FRCs alone or FRCs co-cultured with MFC cells, and different treatments of TNS4 silencing in MFC cells or ITGB1 silencing in FRCs, we found that knockdown of TNS4 or knockdown of ITGB1 could reduce the expression of TGF-β pathway related molecules such as p-SMAD2, p-SMAD3, TGF-β1, and p-AKT caused by tumor cell-FRCs interaction, and simultaneously knockdown of TNS4/ITGB1 can synergize the inhibitory effects on these molecules (Fig. 5A **and B**). Furthermore, to confirm the contribution of the TGF-β1 pathway, TGF-β1 neutralizing antibody was used to treat FRCs which were co-cultured with MFC cells. It was found that TGF-β1 neutralization could reduce the expression of p-SMAD2 or p-SMAD3, and further synergized the inhibitory effects of TNS4 or ITGB1 knockdown on TGF-β pathway related molecules (Fig. 5C **and D**). These results suggested that TNS4 may interact with ITGB1 on FRCs, thereby affecting the binding of TGF-β1 to ITGB1 and subsequently regulating the expression of a series of downstream signaling molecules (Fig. 5E).

Targeting TNS4 - ITGB1 axis suppresses GC cell-induced LN metastasis and TGF-β1 related signaling

To further validate the above results, we used the shRNA of TNS4 and the inhibitor of ITGB1 to detect the effects of TNS4 - ITGB1 axis in GC-induced LN metastasis in vivo (Fig. 6A). Groups were set as: MFC-vehicle group, MFC-sh-TNS4 group, inhibitor group and MFC-sh-TNS4 + inhibitor group. It was found that the knockdown of TNS4 or inhibition of ITGB1 could suppress the expansion of DLNs induced by the tumor cell invasion, compare to control (MFC-vehicle) group. Simultaneously inhibition of TNS4 and ITGB1 could significantly suppress the expansion of DLNs (Fig. 6B). Statistical analyses also indicated that knockdown of TNS4 or inhibition of ITGB1, especially inhibition of both TNS4 and ITGB1 could suppress the increase of LN volume and weight induced by the tumor cell invasion (Fig. 6C **and D**).

By IHC staining of those mouse DLN tissues, we found that knockdown of TNS4 or inhibition of ITGB1, especially inhibition of both TNS4 and ITGB1 could suppress the invasion of MFC cells (Fig. 6E). Through western blotting detection of DLN tissues after the administration of TNS4 shRNA and ITGB1 inhibitor, we further found that knockdown of TNS4 or inhibition of ITGB1 could reduce the expression of p-SMAD2, p-SMAD3, TGF-β1, and p-AKT caused by tumor cell-FRCs interaction, and simultaneously inhibition of TNS4/ITGB1 can synergize the inhibitory effects on these molecules (Fig. 6F and G). Our results indicated that TNS4 could interact with ITGB1 on FRCs, thereby affecting the binding of TGF-β1 to ITGB1 and subsequently regulating downstream signaling molecules, thus supporting the GC cell-induced LN metastasis (Fig. 6H).

Discussion

LNs are important immune regulatory organs and play a crucial role in various tumor metastatic processes. During the process of tumor cell-induced LN metastasis, the stromal cell within the LNs is one of the first cells to respond to the tumor cell invasion, in which FRCs take up a large part. FRCs have been reported as intrinsic mesenchymal cells in LN, capable of secreting extracellular matrix (ECM) to form a network connecting with nerve fibers and immune cells in LNs [25, 26]. Multiple studies have shown that the expansion of LNs induced by infection or tumor cell invasion is mainly regulated by FRCs[27–29].

FRCs regulation is mainly involved in the change of cellular biomechanical properties, which largely depends on the interaction between FRCs and DC cells through PDPN-CLEC-2. Moreover, the proliferation of FRCs leads to LN expansion, accompanied by the proliferation of lymphocytes and the differentiation of various immune cells into inhibitory types, thereby reshaping a microenvironment suitable for tumor cell invasion and growth [30, 31]. Therefore, the communication between tumor cells and FRCs in LNs is a key research object for LN metastasis in various tumors, including GC.

Recent reports have shown that fibroblasts can adhere to ECM molecules through ITGB1, thus participating in biological processes such as cell migration, proliferation and transformation. In addition, ITGB1 can interact with various extracellular signaling molecules and intracellular signaling pathways to regulate the activation status

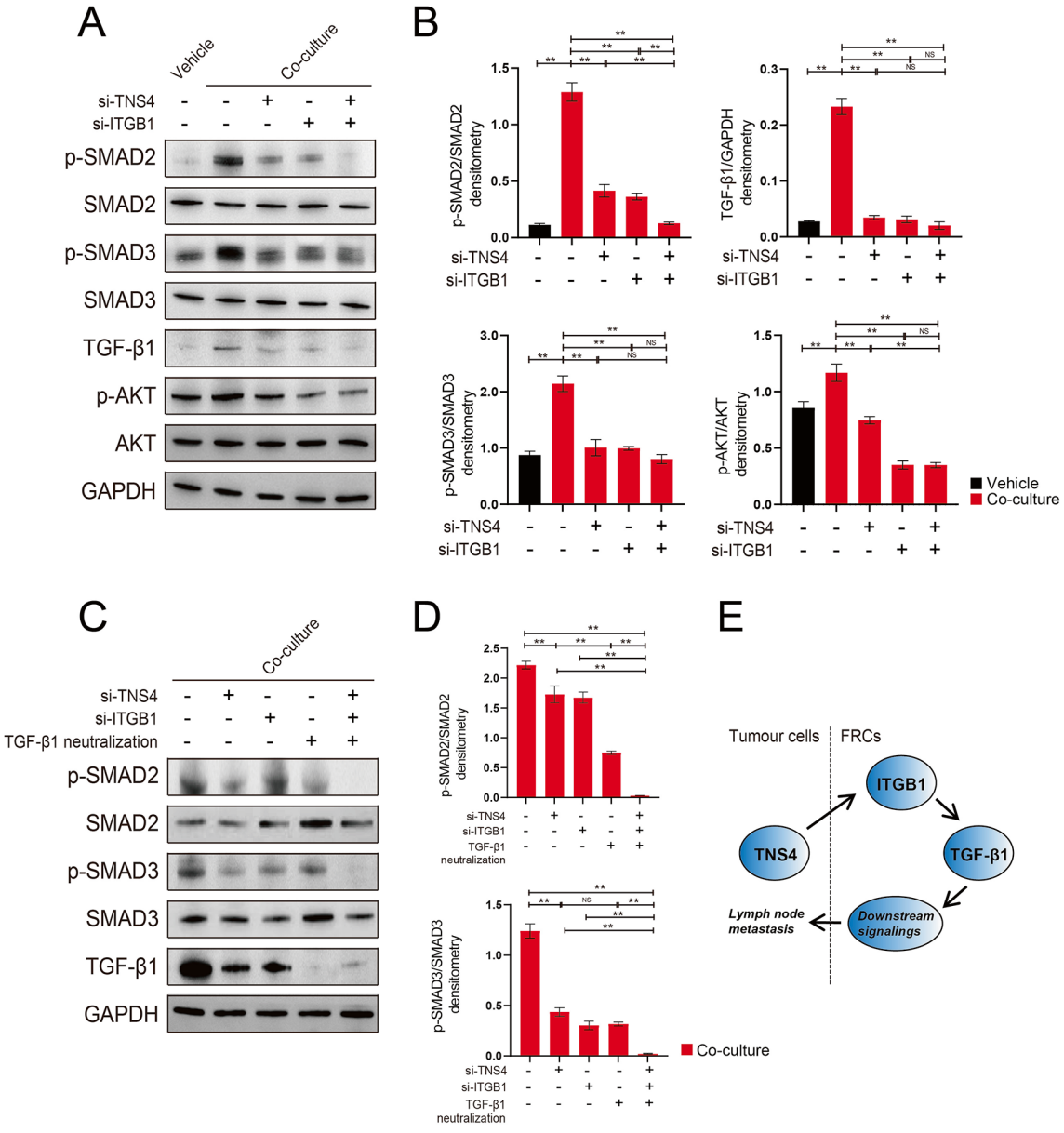

Fig. 5 TNS4-ITGB1 regulated ITGB1 dependent TGF-β1-related signaling pathway. (**A** and **B**). Changes of signaling pathway molecules such as p-SMAD2, SMAD2, p-SMAD3, SMAD3, TGF-β1, p-AKT and AKT in FRCs alone and FRCs co-cultured with MFC cells respectively, with knockdown of TNS4 in MFC cells or knockdown of ITGB1 in FRCs (**A**). The results of the densitometry analyses are shown on the right (**B**). Data were presented as the means ± SD ($n = 3$); (**C** and **D**).Changes of p-SMAD2, SMAD2, p-SMAD3, SMAD3 and TGF-β1 in FRCs co-cultured with MFC cells, with knockdown of TNS4 in MFC cells or knockdown of ITGB1 in FRCs and administration of TGF-β1 neutralizing antibody (**C**). The results of the densitometry analyses are shown on the right (**D**). Data were presented as the means ± SD ($n = 3$); (**E**). Hypothesis on the interaction between TNS4 - ITGB1 - TGF-β1. *$P < 0.05$;** $P < 0.01$;NS: no significance

of fibroblasts [32, 33]. Notably, the interaction between ITGB1 and TGF-β1 can activate downstream signaling pathway molecules of TGF-β1, thus affecting a series of cellular biological processes, including the activation of fibroblasts [34]. Therefore, the expression level and function of ITGB1 have a significant impact on the activated status of fibroblasts, including FRCs.

This study reveals that interfering with TNS4 can inhibit LN metastasis and activation of FRCs in LN tissues of GC, thereby inhibiting LN expansion. Further in-depth research showed that TNS4 derived from tumor cells located at the forefront of LN invasion can interact with ITGB1 on FRCs, causing the release of TGF-β1 and activating downstream signaling pathway molecules, thus activating and reshaping the microenvironment favorable for tumor cell growth in LNs. Therefore, TNS4 is confirmed to have an important regulatory effect on the TGF-β1 signaling pathway through its interaction

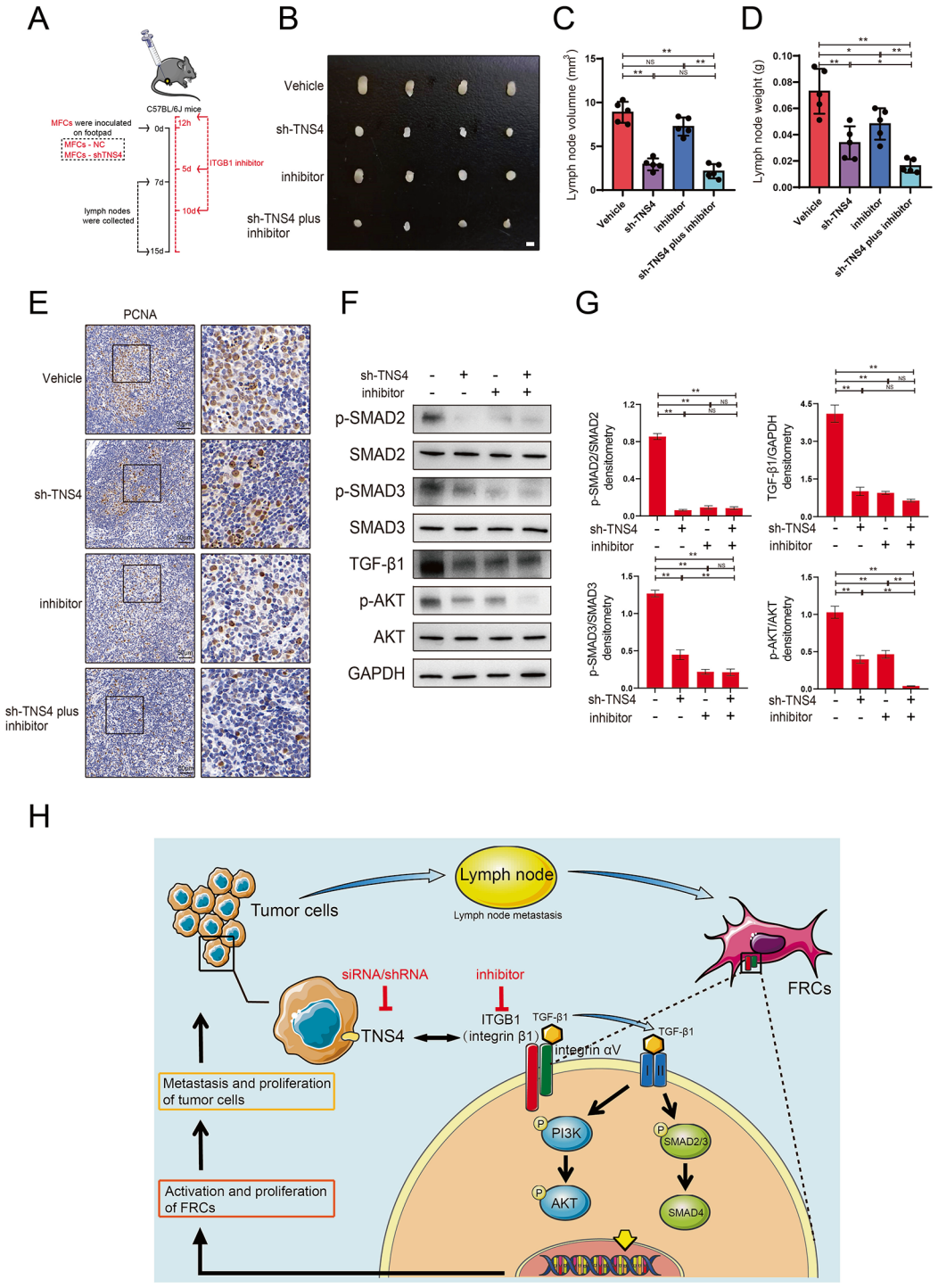

Fig. 6 Blocking of TNS4-ITGB1 axis inhibits the metastasis of tumor cells and TGF-β1-related signaling. (**A**). The construction process of a mouse foot pad model using ITGB1 inhibitor in combination with TNS4 interference; (**B**). The morphological changes of LN tissues from mice in the control group, TNS4 silenced group, ITGB1 inhibitor-treated group and TNS4 shRNA/ITGB1 inhibitor treated group at 15 days. Scale Bar: 1 mm; (**C** and **D**). The changes of the volume (**C**) and weight (**D**) of LN tissues in the control group, TNS4 silenced group, ITGB1 inhibitor-treated group and TNS4 shRNA/ITGB1 inhibitor-treated group at 15 days; (**E**). IHC staining of PCNA in LN tissues of the control group, TNS4 silenced group, ITGB1 inhibitor-treated group and TNS4 shRNA/ITGB1 inhibitor-treated group at 15 days; (**F** and **G**). Changes of p-SMAD2, SMAD2, p-SMAD3, SMAD3, TGF - β1, p-AKT and AKT in LN tissues of the control group, TNS4 silenced group, ITGB1 inhibitor-treated group and TNS4 shRNA/ITGB1 inhibitor-treated group at 15 days. The results of the densitometry analyses are shown on the right (**G**). Data were presented as the means ± SD ($n = 3$); (**H**). TNS4 regulates the TGF-β1 signaling pathway by interacting with ITGB1, affecting the activation of FRCs in LNs and promoting LN metastasis of GC cells. * $P < 0.05$;** $P < 0.01$;NS: no significance

with ITGB1, affecting the activation of FRCs in LNs and reshaping the microenvironment, thereby promoting LN metastasis in GC cells.

Supplementary Information

The online version contains supplementary material available at https://doi.org/10.1186/s12935-025-03830-x.

Supplementary material-abbreviations

Supplementary Table 1

Supplementary Table 2

Supplementary Figure 1

Acknowledgements
We thank Dr. Xiao-Mei Yang, Dr. Yan-Li Zhang, Dr. Lei Zhu, and Dr. Lin-Li Yao for assistance with our experiments.

Author contributions
X.Z., J.L. and J.X. designed and supervised the overall study, analyzed data, and drafted the manuscript. X.Z. and G.-H.S. constructed the mouse footpad model and collected the LN tissues. T.-S.B., W.-P.H., Y.-Y.W., and Y.-Q.Z. assisted with analysis of IHC and IF staining. J.-X.X., F.W. and H.L. analyzed the RNA-seq data. R.L., S.Z., S.-Q.Y., Q.L. and S.-H.J. technically assisted with experiments and analyzed data. X.Z., J.L. and J.X. supervised this study and edited the manuscript.

Funding
This study was supported by the National Natural Science Foundation of China (ID 82073023, 81871923, to J. Li; ID 82372821, 82103357 to L.-P. Hu; ID 82002485, to Q. Li; ID 82103348, to Y.Y. Wang), the Natural Science Foundation of Shanghai (ID 21ZR1461300 to L.-P. Hu), Shanghai Science and Technology Commission Sailing Project (ID 21YF1445200 to L.-P. Hu).

Data availability
The RNA-seq data from this study have been deposited on the NCBI (http://www.ncbi.nlm.nih.gov/) database under the umbrella BioProject PRJNA1160027.

Declarations

Ethics approval and consent to participate
The study was approved by the Research Ethics Committee of Renji Hospital, School of Medicine, Shanghai Jiao Tong University. All participants in the study provided informed consent before specimens were collected. Approval letter of Shanghai Jiaotong University School of Medicine, Renji Hospital Ethics Committee is KY2024-046-C. The animal experiments were approved by the Renji Hospital Animal Ethics Committee (ID: 2024-066).

Competing interests
The authors declare no competing interests.

Received: 14 October 2024 / Accepted: 15 May 2025
Published online: 06 June 2025

References

1. Siegel RL, Miller KD, Jemal A. Cancer statistics, 2020. Ca-a Cancer J Clin. 2020;70:7–30.
2. Arnold M, Park JY, Camargo MC, et al. Is gastric cancer becoming a rare disease? A global assessment of predicted incidence trends to 2035. Gut. 2020;69:823–9.
3. Zeng YJ, Jin RU. Molecular pathogenesis, targeted therapies, and future perspectives for gastric cancer. Sem Cancer Biol. 2022;86:566–82.
4. Wang YY, Zhou YQ, Xie JX, et al. MAOA suppresses the growth of gastric cancer by interacting with NDRG1 and regulating the Warburg effect through the PI3K/AKT/mTOR pathway. Cell Oncol. 2023;46:1429–44.
5. Ni B, He X, Zhang YQ, et al. Tumor-associated macrophage-derived GDNF promotes gastric cancer liver metastasis via a GFRA1-modulated autophagy flux. Cell Oncol. 2023;46:315–30.
6. Jiang Q, Chen H, Zhou SX, et al. Ubiquilin-4 induces immune escape in gastric cancer by activating the Notch signaling pathway. Cell Oncol. 2024;47:303–19.
7. Akiyama Y, Katai H, Kitabayashi R, et al. Frequency of lymph node metastasis according to tumor location in clinical T1 early gastric cancer: supplementary analysis of the Japan clinical oncology group study (JCOG0912). J Gastroenterol. 2023;58:519–26.
8. Tanizawa Y, Terashima M. Lymph node dissection in the resection of gastric cancer: review of existing evidence. Gastric Cancer. 2010;13:137–48.
9. Yamashita K, Hosoda K, Ema A, et al. Lymph node ratio as a novel and simple prognostic factor in advanced gastric cancer. Ejso. 2016;42:1253–60.
10. de Jongh C, Triemstra L, van Der Veen A, et al. Pattern of lymph node metastases in gastric cancer: a side-study of the multicenter LOGICA-trial. Gastric Cancer. 2022;25:1060–72.
11. Sexton RE, Al Hallak MN, Diab M, et al. Gastric cancer: a comprehensive review of current and future treatment strategies. Cancer Metastasis Rev. 2020;39:1179–203.
12. Johnston FM, Beckman M. Updates on management of gastric Cancer. Curr Oncol Rep 2019;21.
13. Nishino T, Sasaki N, Chihara M, et al. Distinct distribution of the tensin family in the mouse kidney and small intestine. Exp Anim. 2012;61:525–32.
14. Clark K, Howe JD, Pullar CE, et al. Tensin 2 modulates cell contractility in 3D collagen gels through the RhoGAP DLC1. J Cell Biochem. 2010;109:808–17.
15. Touaitahuata H, Morel A, Urbach S, et al. Tensin 3 is a new partner of Dock5 that controls osteoclast podosome organization and activity. J Cell Sci. 2016;129:3449–61.
16. Seo EY, Jin SP, Kim YK, et al. Integrin-β4-TNS4-Focal adhesion kinase signaling mediates keratinocyte proliferation in human skin. J Invest Dermatology. 2017;137:763–6.
17. Raposo TP, Alfahed A, Nateri AS, et al. Tensin4 (TNS4) is upregulated by Wnt signalling in adenomas in multiple intestinal neoplasia (Min) mice. Int J Exp Pathol. 2020;101:80–6.
18. Mainsiouw L, Ryan ME, Hafizi S, et al. The molecular and clinical role of tensin 1/2/3 in cancer. J Cell Mol Med. 2023;27:1763–74.
19. Qian XL, Li GR, Vass WC, et al. The Tensin-3 protein, including its SH2 domain, is phosphorylated by Src and contributes to tumorigenesis and metastasis. Cancer Cell. 2009;16:246–58.
20. Shi ZZ, Wang WJ, Chen YX et al. The miR-1224-5p/TNS4/EGFR axis inhibits tumour progression in oesophageal squamous cell carcinoma. Cell Death Dis 2020;11.
21. Di-Luoffo M, Pirenne S, Saandi T, et al. A mouse model of cholangiocarcinoma uncovers a role for Tensin-4 in tumor progression. Hepatology. 2021;74:1445–60.
22. Lee CK, Jeong SH, Jang C, et al. Tumor metastasis to lymph nodes requires YAP-dependent metabolic adaptation. Science. 2019;363(6427):644–9.
23. Zhou YQ, Bao TS, Xie JX, et al. The SLITRK4-CNPY3 axis promotes liver metastasis of gastric cancer by enhancing the endocytosis and recycling of TrkB in tumour cells. Cell Oncol. 2023;46:1049–67.
24. Li J, Xu CJ, Tian GA, et al. Spatiotemporal quantification of metastatic tumour cell growth and distribution in lymph nodes by whole-mount tissue 3D imaging. Int J Biol Sci. 2022;18:3993–4005.
25. Rodda LB, Lu E, Bennett ML, et al. Single-Cell RNA sequencing of lymph node stromal cells reveals Niche-Associated heterogeneity. Immunity. 2018;48:1014–.
26. Li LS, Wu J, Abdi R, et al. Lymph node fibroblastic reticular cells steer immune responses. Trends Immunol. 2021;42:723–34.
27. Martinez VG, Pankova V, Krasny L, et al. Fibroblastic reticular cells control conduit matrix deposition during lymph node expansion. Cell Rep. 2019;29:2810–.
28. Pezoldt J, Wiechers C, Zou MG et al. Postnatal expansion of mesenteric lymph node stromal cells towards reticular and CD34 stromal cell subsets. Nat Commun 2022;13.
29. Chyou S, Ekland EH, Carpenter AC, et al. Fibroblast-type reticular stromal cells regulate the lymph node vasculature. J Immunol. 2008;181:3887–96.

30. Astarita JL, Cremasco V, Fu JX, et al. The CLEC-2-podoplanin axis controls the contractility of fibroblastic reticular cells and lymph node microarchitecture. Nat Immunol. 2015;16:75–.
31. Acton SE, Farrugia AJ, Astarita JL, et al. Dendritic cells control fibroblastic reticular network tension and lymph node expansion. Nature. 2014;514:498–.
32. Zheng XB, Wang P, Li L et al. Cancer-Associated fibroblasts promote vascular invasion of hepatocellular carcinoma via downregulating Decorin-integrin B1 signaling. Front Cell Dev Biology 2021;9.
33. Zonouzi SK, Pezeshki PS, Razi S, et al. Cancer-associated fibroblasts in colorectal cancer. Clin Translational Oncol. 2022;24:757–69.
34. Li Y, Liu C, Li BS, et al. Electrical stimulation activates Calpain 2 and subsequently upregulates collagens via the integrin β1/TGF-β1 signaling pathway. Cell Signal. 2019;59:141–51.

Publisher's note